

Parameters Variability Effects on Multiconductor Interconnects via Hermite Polynomial Chaos

*Original*

Parameters Variability Effects on Multiconductor Interconnects via Hermite Polynomial Chaos / Stievano, IGOR SIMONE; Manfredi, Paolo; Canavero, Flavio. - In: IEEE TRANSACTIONS ON COMPONENTS, PACKAGING, AND MANUFACTURING TECHNOLOGY. - ISSN 2156-3950. - STAMPA. - 1:8(2011), pp. 1234-1239.  
[10.1109/TCPMT.2011.2152403]

*Availability:*

This version is available at: 11583/2418725 since:

*Publisher:*

IEEE

*Published*

DOI:10.1109/TCPMT.2011.2152403

*Terms of use:*

This article is made available under terms and conditions as specified in the corresponding bibliographic description in the repository

*Publisher copyright*

(Article begins on next page)

# Parameters Variability Effects on Multiconductor Interconnects via Hermite Polynomial Chaos

Igor S. Stievano, *Senior Member, IEEE* Paolo Manfredi, *Student Member, IEEE*,  
Flavio G. Canavero, *Fellow, IEEE*,

**Abstract**—This paper focuses on the derivation of an enhanced transmission-line model allowing for the stochastic analysis of a realistic multiconductor interconnect. The proposed model, that is based on the expansion of the well-known telegraph equations in terms of orthogonal polynomials, includes the variability of geometrical or material properties of the interconnect due to uncertainties like fabrication process or temperature. A real application example involving the frequency-domain analysis of a coupled microstrip and the computation of the parameters variability effects on the transmission-line response concludes the paper.

**Index Terms**—Circuit modeling, Circuit Simulation, Transmission-lines, Stochastic analysis, Tolerance analysis, Uncertainty, Polynomial Chaos.

## I. INTRODUCTION

Recently, the interest has grown in developing simulation techniques for the analysis of high-speed digital links with the inclusion of the effects of possible uncertainties of the circuit parameters. A relevant example is provided by the process-induced variability that unavoidably impacts on the system performance and that becomes one of the major concerns for setting realistic design margins. In this framework, the availability of a tool during the early design phase for the stochastic analysis of a digital link is highly desirable.

The typical resource allowing to collect quantitative information on the statistical behavior of the circuit response is based on the application of the brute-force Monte Carlo (MC) method, or possible complementary methods based on the optimal selection of the subset of model parameters in the whole design space [1]. Such methods, however, are computationally expensive, and this fact prevents us from their application to the analysis of complex realistic structures.

An effective solution that overcomes the previous limitation, has been proposed. This methodology is based on the so-called polynomial chaos (PC) theory [2], [3], [4] and on the representation of the stochastic solution of a dynamical circuit in terms of orthogonal polynomials. This technique enjoys applications in several domains of Physics; we limit ourselves to mention recent results on the extension of the classical circuit analysis tools, like the modified nodal analysis (MNA), to the prediction of the stochastic behavior of circuits with uncertain parameters [5], [6], [7], [8]. However, so far, the application has been limited to dynamical circuits consisting only of lumped elements.

Igor Stievano, Paolo Manfredi and Flavio Canavero are with Dipartimento di Elettronica, Politecnico di Torino, 10129 Torino, Italy (e-mail: {igor.stievano,paolo.manfredi,flavio.canavero}@polito.it).

In this paper, the modeling of circuit elements via the PC theory is extended to handle the class of long and distributed interconnects described by multiconductor transmission-line equations [9]. In this study, the variability is provided by the uncertainties affecting the guiding structure (e.g., geometrical tolerances and material properties depending on fabrication process, or operating temperature) that are assumed to behave as random variables with Gaussian distribution. This will allow the stochastic analysis of realistic structures combining lumped circuits and distributed interconnects, as required by the simulation of high-speed digital links.

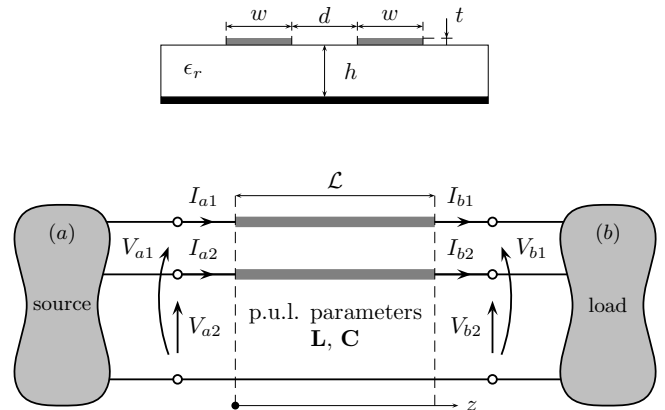


Fig. 1. Test structure considered to demonstrate the proposed approach. Top panel: cross-section; bottom panel: simulation test case.

## II. STOCHASTIC TRANSMISSION-LINE EQUATIONS

This section discusses the modification to the transmission-line equations, allowing to include the effects of the statistical variation of the per-unit-length (p.u.l.) parameters via the PC theory. For the sake of simplicity, the discussion is based on a lossless multiconductor transmission-line as the coupled line structure shown in Fig. 1 with the relative dielectric constant  $\epsilon_r$  and the separation  $d$  that are assumed to be defined by

$$\begin{cases} \epsilon_r &= \bar{\epsilon}_r(1 + \sigma_1\xi_1) \\ d &= \bar{d}(1 + \sigma_2\xi_2) \end{cases} \quad (1)$$

where  $\xi_1$  and  $\xi_2$  are independent Gaussian random variables with zero mean value and unit variance,  $\bar{\epsilon}_r$  and  $\bar{d}$  are the mean values of the parameters and  $\sigma_1$  and  $\sigma_2$  are the corresponding normalized standard deviations.

The extension of the proposed technique to different multi-conductor structures that possibly include losses and to a larger number of random variables is straightforward.

#### A. Deterministic model

The electrical behavior in frequency-domain of the line of Fig. 1 is described by the well-known telegraph equations,

$$\frac{d}{dz} \begin{bmatrix} \mathbf{V}(z, s) \\ \mathbf{I}(z, s) \end{bmatrix} = -s \begin{bmatrix} 0 & \mathbf{L} \\ \mathbf{C} & 0 \end{bmatrix} \begin{bmatrix} \mathbf{V}(z, s) \\ \mathbf{I}(z, s) \end{bmatrix} \quad (2)$$

where  $s$  is the Laplace variable,  $\mathbf{V} = [V_1(z, s), V_2(z, s)]^T$  and  $\mathbf{I} = [I_1(z, s), I_2(z, s)]^T$  are vectors collecting the voltage and current variables along the multiconductor line ( $z$  coordinate) and  $\mathbf{C}$  and  $\mathbf{L}$  are the p.u.l. capacitance and inductance matrices depending on the geometrical and material properties of the structure [9].

#### B. Hermite polynomial chaos

In order to account for the uncertainties affecting the guiding structure, we must consider the p.u.l. matrices  $\mathbf{C}$  and  $\mathbf{L}$  as random quantities, with entries depending on the random vector  $\boldsymbol{\xi} = [\xi_1, \xi_2]^T$ . In turn, (2) becomes a stochastic differential equation, leading to randomly-varying voltages and currents along the line.

A powerful tool allowing to solve in a clever way stochastic equations is the so-called Hermite PC [3]. The idea behind this technique is the spectral expansion of a random variable in terms of a truncated series of Hermite polynomials that are functions of the random vector  $\boldsymbol{\xi}$ . These polynomials play the same role as sinusoidal functions in the Fourier series expansion. Table I collects the basic definitions and properties of Hermite polynomials.

For the current application, the random p.u.l. matrices in (2) are represented through the Hermite expansion as follows,

$$\mathbf{C} = \sum_{k=0}^P \mathbf{C}_k \cdot \phi_k(\boldsymbol{\xi}), \quad \mathbf{L} = \sum_{k=0}^P \mathbf{L}_k \cdot \phi_k(\boldsymbol{\xi}) \quad (3)$$

where  $\{\mathbf{C}_k\}$  and  $\{\mathbf{L}_k\}$  are the expansion coefficients with respect to the orthogonal components  $\{\phi_k\}$  defined in Tab. II.

It should be remarked that the entries of the p.u.l. capacitance and inductance matrices of (2) are nonlinear functions the geometrical and material parameters defining the structure. Each entry of the matrices  $\mathbf{C}$  and  $\mathbf{L}$  can be considered as known nonlinear function of the random vector  $\boldsymbol{\xi}$ , playing the same role of the parameter  $Y(\boldsymbol{\xi})$  of Tab. I. Thus, the expansion coefficients of the above matrices can be computed according to the projection operation defined in Tab. I. Additional details on the computation of the expansion matrices  $\mathbf{C}_k$  and  $\mathbf{L}_k$  for a realistic test case are given in Sec. III and in the Appendix (e.g., see eq. (15)).

For a given number of random variables  $n$  and order  $p$  of the expansion (that corresponds to the highest order of the polynomials in (3) and generally lies within the range from

two to five for practical applications), the total number of terms is

$$(P+1) = \frac{(n+p)!}{n!p!} \quad (4)$$

that turns out to be equal to ten for the case  $n = 2$  and  $p = 3$ .

Readers are referred to [2], [3] and references therein for a comprehensive and formal discussion of polynomial chaos, including the formulae for the computation of the Hermite polynomials of Tab. II for an arbitrary number of random variables and expansion order.

TABLE I  
HERMITE POLYNOMIAL CHAOS DEFINITIONS AND PROPERTIES.

Object	e.g., parameter $Y$ that depends on $\boldsymbol{\xi} = [\xi_1, \xi_2, \dots, \xi_n]^T$
Expansion	$Y(\boldsymbol{\xi}) = \sum_{k=0}^P Y_k \cdot \phi_k(\boldsymbol{\xi})$
Orthogonal basis	Hermite polynomials $\{\phi_k(\boldsymbol{\xi})\}$ (e.g., see Tab. II for the case $n = 2$ )
Inner product	$\langle \phi_k, \phi_j \rangle = \int_{\mathbb{R}^n} \phi_k(\boldsymbol{\xi}) \phi_j(\boldsymbol{\xi}) W(\boldsymbol{\xi}) d\boldsymbol{\xi}$
Weighting function	$W(\boldsymbol{\xi}) = \frac{1}{\sqrt{(2\pi)^n}} \exp(-\frac{1}{2} \boldsymbol{\xi}^T \boldsymbol{\xi})$
Orthogonality	$\langle \phi_k, \phi_j \rangle = \langle \phi_k^2 \rangle \delta_{kj}$
Expansion coefficients	$Y_k = \langle Y, \phi_k \rangle / \langle \phi_k^2 \rangle$
Mean	$Y_0$

TABLE II  
HERMITE POLYNOMIALS FOR THE CASE OF TWO RANDOM VARIABLES ( $n = 2$ ,  $\boldsymbol{\xi} = [\xi_1, \xi_2]^T$ ) AND A THIRD ORDER EXPANSION ( $p = 3$ ).

index $k$	order $p$	$k$ -th basis $\phi_k$	$\langle \phi_k^2 \rangle$
0	0	1	1
1	1	$\xi_1$	1
2	1	$\xi_2$	1
3	2	$\xi_1^2 - 1$	2
4	2	$\xi_1 \xi_2$	1
5	2	$\xi_2^2 - 1$	2
6	3	$\xi_1^3 - 3\xi_1$	6
7	3	$\xi_1^2 \xi_2 - \xi_2$	2
8	3	$\xi_1 \xi_2^2 - \xi_1$	2
9	3	$\xi_2^3 - 3\xi_2$	6

#### C. Stochastic model

For a predefined order (e.g.,  $p = 1$ ), the use of equation (3), along with a similar expansion of the unknown voltage and current variables, yields a modified version of (2), whose second row is provided below in extended form, as an exemplification

$$\begin{aligned} \frac{d}{dz}(\mathbf{I}_0(z, s)\phi_0(\boldsymbol{\xi}) + \mathbf{I}_1(z, s)\phi_1(\boldsymbol{\xi}) + \mathbf{I}_2(z, s)\phi_2(\boldsymbol{\xi})) = \\ -s(\mathbf{C}_0\phi_0(\boldsymbol{\xi}) + \mathbf{C}_1\phi_1(\boldsymbol{\xi}) + \mathbf{C}_2\phi_2(\boldsymbol{\xi}))(\mathbf{V}_0(z, s)\phi_0(\boldsymbol{\xi}) + \\ + \mathbf{V}_1(z, s)\phi_1(\boldsymbol{\xi}) + \mathbf{V}_2(z, s)\phi_2(\boldsymbol{\xi})) \end{aligned} \quad (5)$$

where the interpretation of the new variables is straightforward.

Projection of (5) on the first three Hermite polynomials leads to the following set of equations, where the argument  $(z, s)$  of the voltage and current variables has been neglected for notation convenience

$$\begin{aligned} \frac{d}{dz}(\mathbf{I}_0\langle\phi_0, \phi_j\rangle + \mathbf{I}_1\langle\phi_1, \phi_j\rangle + \mathbf{I}_2\langle\phi_2, \phi_j\rangle) \\ = -s(\mathbf{C}_0\langle\phi_0^2, \phi_j\rangle\mathbf{V}_0 + \mathbf{C}_0\langle\phi_0\phi_1, \phi_j\rangle\mathbf{V}_1 + \\ + \dots + \mathbf{C}_2\langle\phi_2^2, \phi_j\rangle\mathbf{V}_2), \quad j = 0, 1, 2. \end{aligned} \quad (6)$$

The above equation, along with the companion relation arising from the first row of (2), can be further simplified by using the orthogonality relations of Tab. I for the computation of the inner products  $\langle\phi_k, \phi_j\rangle$  and  $\langle\phi_k\phi_l, \phi_j\rangle$ , leading to the following augmented system, where the random vector  $\boldsymbol{\xi}$  does not appear.

$$\frac{d}{dz} \begin{bmatrix} \tilde{\mathbf{V}}(z, s) \\ \tilde{\mathbf{I}}(z, s) \end{bmatrix} = -s \begin{bmatrix} 0 & \tilde{\mathbf{L}} \\ \tilde{\mathbf{C}} & 0 \end{bmatrix} \begin{bmatrix} \tilde{\mathbf{V}}(z, s) \\ \tilde{\mathbf{I}}(z, s) \end{bmatrix} \quad (7)$$

In the above equation, the new vectors  $\tilde{\mathbf{V}} = [\mathbf{V}_0, \mathbf{V}_1, \mathbf{V}_2]^T$  and  $\tilde{\mathbf{I}} = [\mathbf{I}_0, \mathbf{I}_1, \mathbf{I}_2]^T$  collect the coefficients of the PC expansion of the unknown variables.

It is worth noticing that equation (7) belongs to the same class of (2) and plays the role of the set of equations of an extended multiconductor transmission-line, whose number of conductors is  $(P + 1)$  times larger than in the original line. However, for limited values of  $P$  (as typically occurs in practice) the additional overhead in handling the augmented equations is much less than the time required to run a large number of MC simulations.

#### D. Boundary conditions and simulation

For the deterministic case, the simulation of an interconnect like the one of Fig. 1 amounts to combining the port electrical relations of the two terminal elements defining the source and the load with the transmission-line equation, and solving the system. This is a standard procedure as illustrated for example in [9] (see Ch.s 4 and 5). As an example, when a multiport Thevenin equivalent (defined by a voltage source vector  $\mathbf{E}$  and a series impedance matrix  $\mathbf{Z}_S$ ) and an impedance matrix ( $\mathbf{Z}_L$ ) are used to describe block (a) and block (b) of Fig. 1, respectively, the port equations of the terminations in the Laplace domain become

$$\begin{cases} \mathbf{V}_a(s) = \mathbf{E}(s) - \mathbf{Z}_S(s)\mathbf{I}_a(s) \\ \mathbf{V}_b(s) = \mathbf{Z}_L(s)\mathbf{I}_b(s) \end{cases} \quad (8)$$

where the port voltages and currents need to match the solutions of the differential equation (7) at line ends (e.g.,  $\mathbf{V}_a(s) = \mathbf{V}(z=0, s)$ ,  $\mathbf{V}_b(s) = \mathbf{V}(z=\mathcal{L}, s)$ ).

Similarly, when the problem becomes stochastic, the augmented transmission-line equation (7) is used in place of (2) together with the projection of the characteristics of the source and the load elements (8) on the first  $(P + 1)$  Hermite polynomials. It is worth noticing that in this specific example, no variability is included in the terminations and thus the augmented characteristics of the source and load turn out to have a sparse structure with null contributions of the projection of (8) on the  $k$ -th Hermite polynomials, with  $k > 0$ .

Once the unknown voltage and currents are computed, the quantitative information on the spreading of circuit responses can be readily obtained from the analytical expression of the unknowns. As an example, the frequency-domain solution of the magnitude of voltage  $V_{a1}$  with  $p = 1$ , leads to  $|V_{a1}(j\omega)| = |V_{a10}(j\omega)\phi_0(\boldsymbol{\xi}) + V_{a11}(j\omega)\phi_1(\boldsymbol{\xi}) + V_{a12}(j\omega)\phi_2(\boldsymbol{\xi})|$ . The above relation, that turns out to be a known nonlinear function of the random vector  $\boldsymbol{\xi}$ , can be used to compute the PDF of  $|V_{a1}(j\omega)|$  via numerical simulation or analytical formulae [10].

### III. NUMERICAL RESULTS

In this Section, the proposed technique is applied to the analysis of the coupled microstrip structure of Fig. 1, where  $w = 100 \mu\text{m}$ ,  $h = 60 \mu\text{m}$ ,  $t = 35 \mu\text{m}$  and  $\mathcal{L} = 5 \text{ cm}$ . The source and load elements are defined according to the notation in (8) with

$$\begin{aligned} \mathbf{Z}_S &= R_S \begin{bmatrix} 1 & 0 \\ 0 & 1 \end{bmatrix}, \\ \mathbf{Z}_L &= (G_L + sC_L)^{-1} \begin{bmatrix} 1 & 0 \\ 0 & 1 \end{bmatrix}, \end{aligned} \quad (9)$$

being  $R_S = 50 \Omega$ ,  $G_L = 10^{-4} \text{ S}$  and  $C_L = 10 \text{ pF}$ .

Also, one line is active and the other is quiet and kept in the low state, i.e., the corresponding voltage source at the near-end is zero. As already outlined before the variability is provided by the relative permittivity  $\epsilon_r$  and the trace separation  $d$ , that are assumed to behave as two independent Gaussian random variables with 3.7 and  $80 \mu\text{m}$  mean values, respectively, and identical 10% relative standard deviation. The approximate relations collected in [13], [14], [15] have been used to compute the third-order PC expansion of the unknowns and of the p.u.l. parameters of the structure. Additional details on the computation of the expansion matrices defined by (3) are collected in the Appendix.

Figure 2 shows a comparison of the Bode plot (magnitude) of the transfer function  $H(j\omega)$  defining the near-end crosstalk computed via the advocated PC method and determined by means of the MC procedure. The solid black thin curves of Fig. 2 represent the  $\pm 3\sigma$  interval of the transfer function, determined from the results of the proposed technique. For comparison, the deterministic response with nominal values of the circuit elements is reported in Fig. 2 as a solid black thick line; also, a limited set of MC simulations (100, out of the 40,000 runs, in order not to clutter the figure) are plotted as gray lines. Clearly, the thin curves of Fig. 2 provide a qualitative information of the spread of responses due to parameters uncertainty. A better quantitative prediction can be appreciated in Fig. 3, comparing the PDF of  $|H(j\omega)|$  computed for different frequencies with the distribution obtained

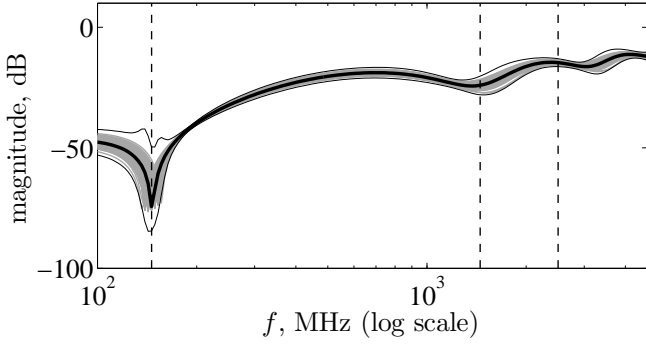


Fig. 2. Bode plots (magnitude) of the near-end crosstalk transfer function  $H(j\omega)$  of the example test case (see text for details). Solid black thick line: deterministic response; solid black thin lines:  $3\sigma$  tolerance limit of the third order polynomial chaos expansion; gray lines: a sample of responses obtained by means of the MC method (limited to 100 curves, for graph readability).

via the analytical PC expansion. The frequencies selected for this comparison correspond to the dashed lines shown in Fig. 2. The good agreement between the actual and the predicted PDFs and, in particular, the accuracy in reproducing the tails and the large variability of non-gaussian shapes of the reference distributions, confirm the potential of the proposed method. For this example, it is also clear that a PC expansion with  $p = 3$  is already accurate enough to capture the dominant statistical information of the system response.

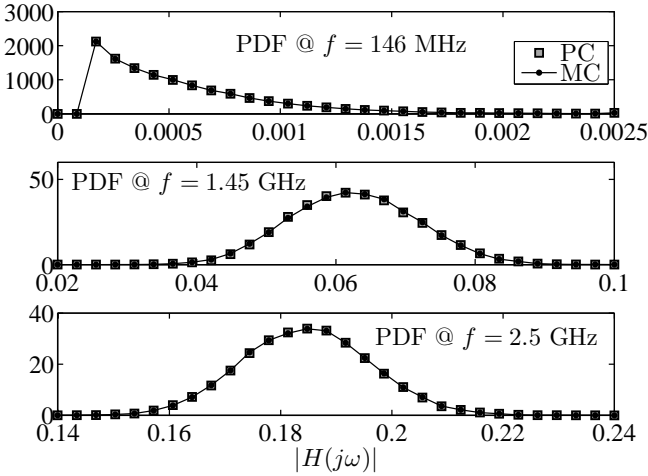


Fig. 3. Probability density function of  $|H(j\omega)|$  for the example of this study, computed at different frequencies. Of the two distributions, the one marked MC refers to 40000 MC simulations, and the one marked PC refers to the response obtained via third order polynomial chaos expansion.

In addition, Fig. 4 shows the surface of  $|H(j\omega)|$  computed at  $f = 2.5$  GHz as a function of the two random variables  $\xi_1$  and  $\xi_2$ , corresponding to relative permittivity and trace separation, respectively. The comparison between the actual surface and the one predicted via the PC method for a predefined order of the expansion is provided as well. The two plots in the figure correspond to a third and a fifth order of the PC expansion, thus highlighting that the expansion order  $p$  can be effectively used to improve the accuracy of the approximation for a wide range of parameter variability.

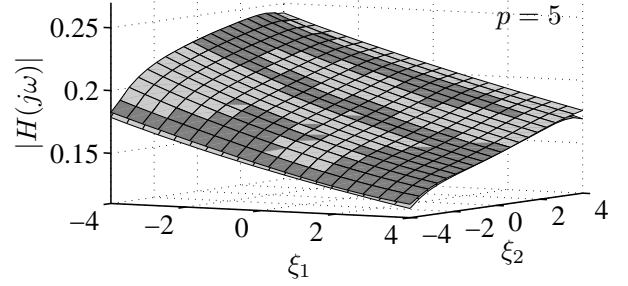
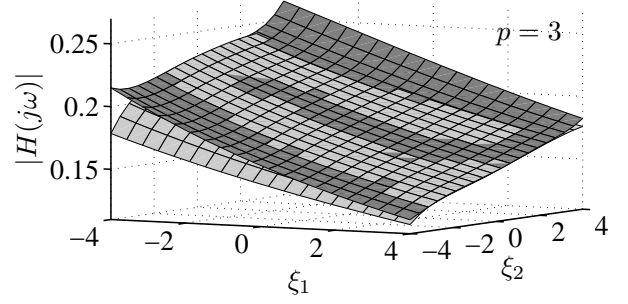


Fig. 4. Plot of  $|H(j\omega)|$  at  $f = 2.5$  GHz as a function of the two random parameters, i.e., the relative permittivity and the trace separation. Light gray: reference; dark gray: PC approximation. The two panels represent the results obtained with different expansion orders (3 and 5).

Finally, Tab. III collects the main figures on the efficiency of the MC and of the proposed PC-based methods implemented in the Matlab<sup>®</sup> environment. The CPU time and memory allocation required by the simulation of the setup of Fig. 1 for the computation of the curves of Fig. 2 are reported in the table. The numbers in the third column represent the memory consumption needed to store the system matrix used by the different methods for a single frequency iteration. For a fair comparison, the fourth column of the table includes the overhead for the construction and solution of the augmented set of transmission-line equations (7), that is only required by the PC method. The above comparison confirms the strengths of PC that allows to generate accurate predictions of the statistical behavior of a realistic interconnect with a great efficiency improvement, with a limited timing and memory overhead.

It is important to remark that the proposed PC technique can be effectively used without any modification of the method for a number of random variables on the order of ten. With a larger number of variables, the computation of the expansion coefficients of (3) requires the solution of multiple integrals (see the definition of the inner product of Tab. I), thus leading to an unavoidable initial overhead that is not negligible. In this case, a clever integration strategy needs to be used. Also, the size of the augmented set of transmission-line equations defined by (7) increases with the number of variables. As an example, a third order expansion for the case of ten random

TABLE III  
CPU TIME REQUIRED BY THE SIMULATION OF THE SETUP OF FIG. 1 BY  
THE MC AND THE PROPOSED PC-BASED METHODS.

Method	Order $p$	Memory	Overhead	Simulation time
MC	-	0.25 kB	0 sec	2h 33 min
PC	3	25 kB	12 sec	1.1 sec
PC	5	110 kB	16 sec	1.3 sec
PC	10	1.1 MB	2 min 49 sec	2.2 sec

variables leads to a system that is 286 times larger. Owing to this, if needed, possible model order reduction techniques can be combined with PC to improve the efficiency of the method, as proposed in [12].

#### IV. CONCLUSIONS

This paper addresses the generation of an enhanced multiconductor transmission-line equation describing a realistic interconnect structure with the inclusion of external uncertainties. The proposed method, that is based on the expansion of the voltage and current variables into a sum of a limited number of orthogonal polynomials, allows to compute the quantitative information on the transmission-line response sensitivity to parameters variability. The advocated technique, while providing accurate results, turns out to be more efficient than alternative state-of-the-art solutions like Monte Carlo. The feasibility and strength of the method have been demonstrated on a realistic PCB coupled microstrip structure with two uncertain parameters described by independent Gaussian random variables.

#### Acknowledgements

The authors wish to acknowledge Prof. Claudio Canuto (Dipartimento di Matematica, Politecnico di Torino, Italy) for the fruitful and stimulating discussions on polynomial chaos.

#### APPENDIX

This Appendix briefly summarizes the formulae used for the computation of the p.u.l. parameters of the coupled line structure of Fig. 1 and of the corresponding PC expansions defined by (3).

Matrices  $\mathbf{C}$  and  $\mathbf{L}$  of (2) are computed from the empirical relations in [13], [14], [15], defining the characteristic impedances of the even and the odd propagation modes of a symmetric coupled line structure:

$$\begin{cases} Z_e = \frac{Z_0 \sqrt{(\varepsilon_{\text{eff},0}/\varepsilon_{\text{eff},e})}}{1 - Z_0/\eta_0 \sqrt{\varepsilon_{\text{eff},0}} Q_4} \\ Z_o = \frac{Z_0 \sqrt{(\varepsilon_{\text{eff},0}/\varepsilon_{\text{eff},o})}}{1 - Z_0/\eta_0 \sqrt{\varepsilon_{\text{eff},0}} Q_{10}} \end{cases} \quad (10)$$

where  $\eta_0 = 377 \Omega$  is the free-space impedance,  $Z_0$  and  $\varepsilon_{\text{eff},0}$  are the characteristic impedance and the effective relative permittivity of the isolated strips, respectively, and  $Q_4$  and  $Q_{10}$  are non-linear functions of the thickness  $t$ , normalized land width ( $w/h$ ) and separation ( $d/h$ ). In the above relations,  $\varepsilon_{\text{eff},e}$  and  $\varepsilon_{\text{eff},o}$  are the effective relative permittivities of the modes, defined by

$$\begin{cases} \varepsilon_{\text{eff},e} = 0.5 (\varepsilon_r + 1) + 0.5 (\varepsilon_r - 1) (1 + 10/v)^{-a_e \cdot b_e} \\ \varepsilon_{\text{eff},o} = [0.5 (\varepsilon_r + 1) + a_o - \varepsilon_{\text{eff},0}] e^{-c_o \cdot (d/h)^{d_0}} + \varepsilon_{\text{eff},0} \end{cases} \quad (11)$$

where  $v$ ,  $a_e$ ,  $b_e$ ,  $a_o$ ,  $c_o$  and  $d_0$  are non-linear functions of  $w/h$ ,  $d/h$  and  $\varepsilon_r$ .

As outlined in [9], the p.u.l matrices can be readily obtained via the following standard transformation

$$\begin{cases} \mathbf{LC}^{-1} = \mathbf{T} \begin{bmatrix} Z_o^2 & 0 \\ 0 & Z_e^2 \end{bmatrix} \mathbf{T}^{-1} \\ \mathbf{LC} = \mathbf{T} \begin{bmatrix} 1/v_o^2 & 0 \\ 0 & 1/v_e^2 \end{bmatrix} \mathbf{T}^{-1} \end{cases} \quad (12)$$

where  $v_o$  and  $v_e$  are the modal propagation velocities defined as the speed of light divided by the square root of the modal effective permittivity and

$$\mathbf{T} = \frac{1}{\sqrt{2}} \begin{bmatrix} -1 & 1 \\ 1 & 1 \end{bmatrix}. \quad (13)$$

From the above equations, the sought for parameters write

$$\begin{cases} \mathbf{C} = \sqrt{(\mathbf{CL}^{-1})(\mathbf{LC})} \\ \mathbf{L} = (\mathbf{LC}^{-1})\mathbf{C} \end{cases}. \quad (14)$$

Once the p.u.l. matrices defined by (14) are known as nonlinear, possibly complex, functions of the geometrical and material properties of the structure, the expansion coefficients of (3) can be obtained via the projection of the matrix entries on the Hermite polynomials according to the properties of Tab. I. As an example, the coefficient  $c_{i,j,k}$  defining the entry  $(i, j)$  of the expansion matrix  $\mathbf{C}_k$  writes

$$c_{i,j,k} = \int_{\mathbb{R}^n} \frac{c_{i,j}(\boldsymbol{\xi}) \phi_k(\boldsymbol{\xi})}{\sqrt{(2\pi)^n}} \exp(-\frac{1}{2} \boldsymbol{\xi}^T \boldsymbol{\xi}) / < \phi_k^2 > \quad (15)$$

where  $c_{i,j}$  is the  $(i, j)$  element of matrix  $\mathbf{C}$ , that turns out to be a function of the random vector  $\boldsymbol{\xi}$  as outlined in Sec. II. It is worth noticing that the projection integral (15) can be effectively calculated by means of readily available numerical techniques, such as the adaptive Simpson or Gauss-Kronrod quadratures (e.g., see the Matlab<sup>®</sup> routines `quad.m` or `quadgk.m`).

#### REFERENCES

- [1] Q. Zhang, J. J. Liou, J. McMacken, J. Thomson, P. Layman, "Development of robust interconnect model based on design of experiments and multiobjective optimization," IEEE Transactions on Electron Devices, Vol. 48, No. 9, pp. 1885 – 1891, Sep. 2001.
- [2] R. G. Ghanen, P. D. Spanos, "Stochastic Finite Elements. A Spectral Approach," Springer-Verlag, 1991 (Ch. 2).
- [3] D. Xiu, G. E. Karniadakis, "The Wiener-Askey polynomial chaos for stochastic differential equations," SIAM, Journal of Sci. Computation, Vol. 24, No. 2, pp. 619–622, 2002.
- [4] B. J. Deusschere et Al., "Numerical challenges in the use of polynomial chaos representations for stochastic processes," SIAM Journal on Scientific Computing, Vol. 26, No. 2, pp. 698–719, 2005.
- [5] Q. Su, K. Strunz, "Stochastic circuit modelling with Hermite polynomial chaos," IET Electronics Letters, Vol. 41, No. 21, Oct. 2005.
- [6] K. Strunz, Q. Su, "Stochastic formulation of SPICE-type electronic circuit simulation using polynomial chaos," ACM Transactions on Modeling and Computer Simulation, Vol. 18, No. 4, Sep. 2008.
- [7] Y. Zou et Al., "Practical implementation of stochastic parametrized model order reduction via Hermite polynomial chaos," Proc. of the 2007 Asia and South Pacific Design Automation Conference, pp. 367–372, 2007.
- [8] I. S. Stievano, F. G. Canavero, "Response Variability of High-Speed Interconnects via Hermite Polynomial Chaos," Proc. of the 14th IEEE Workshop on Signal Propagation on Interconnects, Hildesheim, Germany, pp. 3-6, May 09-12, 2010.
- [9] C. R. Paul, "Analysis of Multiconductor Transmission Lines," Wiley, 1994.
- [10] A. Papoulis, "Probability, Random Variables and Stochastic Processes," 3<sup>rd</sup> edition, McGraw-Hill, 1991.
- [11] C. R. Paul, "Introduction to Electromagnetic Compatibility," 2<sup>nd</sup> edition, Wiley, 2006, p. 201.

- [12] Ning Mi; S.X.-D. Tan; Yici Cai, Xianlong Hong, "Fast Variational Analysis of On-Chip Power Grids by Stochastic Extended Krylov Subspace Method" *IEEE Transactions on Computer-Aided Design of Integrated Circuits and Systems*, Vol. 27, No. 11, pp. 1996–2006, Nov. 2008.
- [13] M. Kirschning, R. H. Jansen, "Accurate Wide-Range Design Equations for the Frequency-Dependent Characteristic of Parallel Coupled Microstrip Lines," *IEEE Transactions on Microwave Theory and Techniques*, Vol. MTT-32, No. 1, pp. 83 - 90, Jan 1984.
- [14] M. Kirschning, R. H. Jansen, "Corrections to Accurate Wide-Range Design Equations for the Frequency-Dependent Characteristics of Parallel Coupled Microstrip Lines," *IEEE Transactions on Microwave Theory and Techniques*, Vol. MTT-33, No. 3, p. 288, Mar 1985.
- [15] E. Hammerstad, O. Jensen, "Accurate Models for Microstrip Computer-Aided Design," *Proc. of the IEEE International Symposium on MTT*, Washington D.C., pp. 407–409, May 1980.